



INSTITUT DE FRANCE
Académie des sciences

Comptes Rendus

Physique

Giovanni Pecci, Gianni Aupetit-Diallo, Mathias Albert, Patrizia Vignolo
and Anna Minguzzi

Persistent currents in a strongly interacting multicomponent Bose gas on a ring


Volume 24, Special Issue S3 (2023), p. 87-99

Online since: 27 July 2023

Part of Special Issue: CNRS Gold Medal Jean Dalibard / *Médaille d'or du CNRS*
Jean Dalibard

Guest editors: Yvan Castin (Laboratoire Kastler Brossel (UMR 8552), Département de physique de l'ENS, Paris, France) and Klaus Mølmer (Institut Niels Bohr, Université de Copenhague, Danemark)

<https://doi.org/10.5802/crphys.157>

 This article is licensed under the
CREATIVE COMMONS ATTRIBUTION 4.0 INTERNATIONAL LICENSE.
<http://creativecommons.org/licenses/by/4.0/>



The Comptes Rendus. Physique are a member of the
Mersenne Center for open scientific publishing
www.centre-mersenne.org — e-ISSN : 1878-1535



CNRS Gold Medal Jean Dalibard / *Médaille d'or du CNRS*
Jean Dalibard

Persistent currents in a strongly interacting multicomponent Bose gas on a ring

Courants persistants dans un gaz de bosons à plusieurs composantes en interaction forte sur un anneau

Giovanni Pecci^{Ⓢ,* ,a}, Gianni Aupetit-Diallo^{*,b}, Mathias Albert^{Ⓢ,* ,b,c}, Patrizia Vignolo^{*,b,c} and Anna Minguzzi^{Ⓢ,* ,a}

^a Université Grenoble-Alpes, CNRS, LPMCM, 38000 Grenoble, France

^b Université Côte d'Azur, CNRS, Institut de Physique de Nice, 06560 Valbonne, France

^c Institut universitaire de France (IUF)

E-mails: giovanni.pecci@lpmcm.cnrs.fr (G. Pecci),

gianni.aupetit-diallo@inphyni.cnrs.fr (G. Aupetit-Diallo),

mathias.albert@inphyni.cnrs.fr (M. Albert), patrizia.vignolo@inphyni.cnrs.fr

(P. Vignolo), anna.minguzzi@lpmcm.cnrs.fr (A. Minguzzi)

Abstract. We consider a two-component Bose–Bose mixture at infinitely strong repulsive interactions in a tightly confining, one-dimensional ring trap and subjected to an artificial gauge field. By employing the Bethe Ansatz exact solution for the many-body wavefunction, we obtain the ground state energy and the persistent currents up to four particles. For each value of the applied flux, we then determine the symmetry of the state under particles exchange. We find that the ground-state energy and the persistent currents display a reduced periodicity with respect to the case of non-interacting particles, corresponding to reaching states with fractional angular momentum per particle. We relate this effect to the change of symmetry of the ground state under the effect of the artificial gauge field. Our results generalize the ones previously reported for fermionic mixtures with both attractive and repulsive interactions and highlight the role of symmetry in this effect.

Résumé. Nous considérons un mélange de bosons à deux composantes en interaction répulsive infiniment forte dans un piège en anneau unidimensionnel à fort confinement et soumis à un champ de jauge artificiel. En utilisant la forme exacte de la fonction d'onde à N corps donnée par l'ansatz de Bethe, nous obtenons l'énergie de l'état fondamental et la valeur des courants persistants jusqu'à quatre particules. Ensuite, en fonction du flux appliqué, nous déterminons quelle est la symétrie de l'état sous l'échange de particules. Nous constatons que l'énergie de l'état fondamental et les courants persistants présentent une périodicité réduite par rapport au cas sans interaction, ce qui correspond à l'obtention d'états avec un moment cinétique fractionnaire par particule. Nous relierions cet effet au changement de symétrie de l'état fondamental sous l'effet du champ de jauge artificiel. Nos résultats généralisent ceux précédemment rapportés pour les mélanges fermioniques avec des interactions attractives ou répulsives et mettent en évidence le rôle de la symétrie dans cet effet.

* Corresponding authors.

Keywords. Ultracold atoms, quantum gases, one-dimensional systems, strong interactions, artificial gauge fields, ring trap, exact many-body solution.

Mots-clés. Atomes froids, gaz quantiques, systèmes unidimensionnels, interactions fortes, champs de jauge artificiels, piège en anneau, solution exacte à N corps.

Funding. We acknowledge support from the Quantum-SOPHA ANR Project N. ANR-21-CE47-0009.

Manuscript received 28 November 2022, revised 23 March 2023, accepted 12 April 2023.

1. Introduction

Ultracold atomic gases are a very versatile system for investigating fundamental physics and for quantum simulation [1–3]. The steady progress in trapping and manipulating cold atoms allows for an unprecedented control on the parameters of the system such as interaction strength, number of particles and components, and geometry [4, 5]. In particular, cold atoms can be confined in one-dimensional potentials of different geometries and subsequently used to experimentally realize [6–9] paradigmatic strongly correlated one-dimensional models [10–14]. One of the main advantages of investigating these systems rely on the wide class of exact methods one can implement. For instance, one-dimensional homogeneous systems interacting via zero range potential can be solved at any interaction strength by means of Bethe Ansatz [12, 15, 16], while models including non-homogeneous confinement can be exactly solved in some specific interaction regimes using different methods [17–19].

In the context of homogeneous systems, quantum gases trapped in a ring-shaped potential are a suitable platform to investigate quantum coherence and transport [20]. These systems can be threaded by an artificial gauge flux [21–23]. The corresponding artificial gauge field can be implemented e.g. by stirring the gas using a barrier [24] or by imprinting a geometrical phase to the gas [25]. The artificial gauge field induces a persistent current of particles flowing in the ring (see e.g. [26–28] for reviews in fermionic and bosonic systems). Persistent currents are a manifestation of quantum coherence of the particles all over the ring. They coincide with supercurrents in the case of superfluid or superconductors, but can also occur in normal fermionic systems, and can be used to probe different phases of the system [29, 30]. In ultracold atomic rings, the persistent current can be experimentally accessed by co-expansion protocols of the gas on the ring and a reference gas at the center. The value and the sign of the current emerges as the result of spiral interferometry analysis [31–36].

In analogy with superconducting rings [37], the persistent current is a periodic function of the external effective flux, whose period is defined as the quantum of flux of the gas [38]. The increase the flux by an amount equal to the quantum of flux corresponds to a change of the value of the total angular momentum and consequently of the current. A reduction of the period of the current as a function of the flux has been predicted both for Fermi and for Bose gases with strong attractive interactions [39–41], and corresponds to *angular momentum fractionalization*, i.e. to the possibility of associating a fractional value of angular momentum per particle. This phenomenon relies on the formation of two-body and many-body bound states, respectively for Fermi and Bose gases, which deeply affect the state of the gas. In particular, the period of the current oscillations as a function of the effective flux is reduced by a factor corresponding to the number of particles giving rise to the bound state: two for attracting fermions forming pairs and $N - 1$ with N being the total number of particles – for attracting bosons forming the quantum equivalent of a bright soliton. A similar phenomenon has been predicted for a multi-component Fermi gas with very large repulsive interactions [42, 43]. In this case, the period of the persistent current oscillations is also reduced by a factor N . However, this phenomenon is not related to the

formation of molecules, rather, it is due to the creation of fermionic spin excitations, i.e spinons, in the ground state at finite flux [42, 43].

In this article, we study a strongly-interacting two-component Bose gas trapped on a ring and threaded by an artificial gauge field. The model is exactly solvable: using the Bethe Ansatz we explicitly obtain the many-body wavefunction, the ground-state energy, and the persistent current at very large interactions up to four particles. In analogy with fermionic mixtures, we find that at large interactions the period of the ground-state energy and of the persistent current as a function of the flux is reduced by a factor equal to the total number of particles. At non-zero flux, such ground-state branches correspond to spin-excited states at zero flux, characterized by a different value of angular momentum. Furthermore, we characterize the symmetry under particle exchange of the ground state at varying values of the effective flux. We find that each ground-state branch has a different symmetry i.e. it is associated to a different Young tableau. We also show that, when the number of low-energy spin excitations exceeds the number of particles, for some values of the flux the ground state may be degenerate and correspond to more than one symmetry under particle exchange. For each of such cases we identify the corresponding Young tableaux.

In the following, after introducing the model and the definitions, we first consider the instructive case of two particles and then we study the more involved case of a mixture of four particles.

2. Model and definitions

We consider a two-component Bose–Bose mixture of N atoms, made of $N - M$ particles in one component (denoted as spin up) and M particles in the other component (denoted as spin down). We focus on the balanced case $M = N/2$. The bosons interact via a delta potential of strength g , taking the case where the interaction strength g of the intra-species interactions is the same as the one of the inter-species interactions. The gas is confined in a one-dimensional ring of radius $R \doteq \frac{L}{2\pi}$, with L being the circumference of the ring. We consider an artificial gauge field, e.g. induced by setting the system in rotation with frequency Ω inducing an effective flux $\Phi = 2\Omega\pi R^2$ flowing through the ring.

The Hamiltonian of the system is:

$$\mathcal{H} = \sum_{j=1}^N \frac{1}{2m} (p_j - m\Omega R)^2 + g \sum_{j<\ell} \delta(x_j - x_\ell) \quad (1)$$

where m is the mass of the particles. In the following, we define the quantities $c \doteq \frac{2m}{\hbar^2} g$ and $\tilde{\Phi} \doteq \frac{\Phi}{\Phi_0}$, where $\Phi_0 = \frac{h}{m}$, to indicate respectively the interaction strength and the reduced flux. The kinetic part of the Hamiltonian can be hence rewritten as $\mathcal{H}_{kin} = \sum_{j=1}^N \frac{1}{2m} (p_j - \frac{2\pi\hbar}{L} \tilde{\Phi})^2$. We also set $\epsilon = \frac{\hbar^2 \pi^2}{mL^2}$ as the energy scale.

This model is integrable at any interaction strength and can be solved exactly using Bethe Ansatz [16, 44, 45]. In each coordinate sector $Q = \{x_{Q(1)} \leq x_{Q(2)} \leq \dots x_{Q(N)}\}$ the wavefunction reads [16]:

$$\Psi(x_{Q(1)} \dots x_{Q(N)}) = \sum_P A_Q(\Lambda_m, k_{P(j)}, c) \exp \left\{ i \sum_P k_{P(j)} x_{Q(j)} \right\}, \quad (2)$$

where the sum is performed over all the possible permutations P in the symmetric group S_N . In Eq.(2) we introduced the amplitudes A_Q , the *spin rapidities* Λ_m with $m = 1..M$, M being the number of spin down particles, and the *charge rapidities* k_j with $j = 1..N$. The two sets of

rapidities fully specify the wavefunction of the system: they can be obtained for each value of $\tilde{\Phi}$ by solving the coupled Bethe equations [44],

$$\begin{cases} Lk_j = 2\pi\mathcal{J}_j + 2\sum_{\ell=1}^N \arctan\left(\frac{k_\ell - k_j}{c}\right) + 2\sum_{m=1}^M \arctan\left(\frac{2(k_j - \Lambda_m)}{c}\right) \\ \sum_{j=1}^N 2\arctan\left(\frac{2}{c}(\Lambda_m - k_j)\right) = 2\pi\mathcal{J}_m + \sum_{n=1}^M 2\arctan\left(\frac{\Lambda_m - \Lambda_n}{c}\right), \end{cases} \quad (3)$$

where we introduced the charge and the spin quantum numbers \mathcal{J}_j and \mathcal{J}_m , which are integers or half-integers respectively if $N - M$ is odd or even. The energy of the system is given by $E(\tilde{\Phi}) = \frac{\hbar^2}{2m}\sum_j(k_j - \frac{2\pi}{L}\tilde{\Phi})^2$ and the total momentum is $P = \hbar\sum_j k_j$.

The choice of the quantum numbers fixes the state of the system. In particular, in the ground state, adjacent quantum numbers are spaced by one unit. They are chosen, for each value of the flux, such that the corresponding rapidities k_j minimize the energy $E(\tilde{\Phi})$ [44, 46, 47].

In this article, we focus on the Tonks–Girardeau (TG) fermionized limit $c \rightarrow \infty$, where the inter-particle interactions are infinitely repulsive. This induces an effective Pauli principles among the particles: the wavefunction of the system vanishes as two particles occupy the same spatial position, still ensuring the preservation of the bosonic symmetry under particle exchange. In the TG regime, the Bethe Ansatz solution of the model is markedly simplified. To describe such limit, we introduce the rescaled spin rapidities $\lambda_m \doteq \frac{2\Lambda_m}{c}$ [16, 47, 48], which we assume to be finite in the limit $c \rightarrow \infty$. In this limit, exploiting the anti-symmetry of the arctangent function, the Bethe equations read:

$$\begin{cases} Lk_j = 2\pi\left(\mathcal{J}_j - \frac{1}{N}\sum_{m=1}^M \mathcal{J}_m\right) \\ 2N\arctan(\lambda_m) = 2\pi\mathcal{J}_m + \sum_{n=1}^M 2\arctan(\lambda_m - \lambda_n). \end{cases} \quad (4)$$

The first equation fixes the energy of the system: in this interaction regime the distribution of the quantum numbers \mathcal{J}_m - thus the spin excitations - affects the total momentum and the kinetic energy. The second equation coincides with the Bethe equations for an isotropic spin chain [47, 49, 50] and does not depend on the charge degree of freedom. The same spin-charge decoupling occurs in the wavefunction (2), where the amplitudes satisfy $\lim_{c \rightarrow \infty} A_Q(\Lambda_m, k_{P(j)}, c) = A_Q(\Lambda_m/c) = A_Q(\lambda_m)$ and explicitly read [16, 47]:

$$A_Q(\lambda_1, \dots, \lambda_M) \propto (-1)^{|Q|} \sum_R \prod_{1 \leq m < n \leq M} \frac{\lambda_{R(m)} - \lambda_{R(n)} - 2i}{\lambda_{R(m)} - \lambda_{R(n)}} \prod_{l=1}^M \left(\frac{\lambda_{R(l)} - i}{\lambda_{R(l)} + i}\right)^{y_{Q(l)}}. \quad (5)$$

In this equation, the integer $y_{Q(l)}$ labels the position of the l^{th} spin down in the coordinate sector Q . The notation $|Q|$ indicates the sign of the permutation linking the coordinate sector Q with the identical coordinate sector defined by $x_1 \leq x_2 \leq \dots \leq x_N$.

The nested structure of the Bethe Ansatz, i.e. the presence of a second set of equation for the spin rapidities λ_s , highlights the role of the spin in our system. If we consider a gas of spinless bosons in the regime $c \rightarrow \infty$, the wavefunction (2) has the same functional form: the differences emerge in the definition of the amplitudes and of the Bethe equations. In particular, since the wavefunction only depends on the charge rapidities, in this interacting regime one has $k_j^{\text{spinless}} = \frac{2\pi}{L}\mathcal{J}_j$, where the quantum numbers follow the same rules we mentioned, provided $M = 0$. This yields amplitudes $A_Q^{\text{spinless}} = \pm 1$, where the sign is determined by the coordinate sector, and a fully symmetric wavefunction under particle exchange [51].

We stress that, up to a normalization constant, Eq. (5) has the same functional structure of the Bethe wavefunction of the isotropic Heisenberg spin chain [47, 49, 50]. Despite the same Bethe equations and a similar structure of the spin component of the wavefunction, the expression

for the spectra of Hamiltonian (1) and of the spin chain are in general different: for the full model (1) the energy is given by the charge rapidities, while for the spin chain it is linked to the spin rapidities. Still, the correction to first order in $1/c$ of the spectrum of the full model can be mapped onto the spectrum of the Heisenberg chain by a suitable definition of an effective coupling J of the chain [42, 43].

In order to obtain explicit values for the amplitudes A_Q , we solve the Bethe equations (4) [47, 50] for all the possible distributions of the quantum numbers \mathcal{I}_j and \mathcal{J}_m , which are in turn fixed by the number of particles N and the number of down spins M . Thanks to the periodicity of the Bethe equations, the number of possible sets of quantum numbers yielding independent solutions of Eq. (4) is finite.

In particular, in order to determine the amplitudes of the ground state wavefunction for a fixed value of the flux, we solve the Bethe equation by choosing the sets of quantum numbers that minimize the energy.

The determination of the amplitudes A_Q for each possible spin ordering Q allows us to write explicitly the many-body wavefunction $\Psi(x_{Q(1)} \dots x_{Q(N)})$ in each coordinate sector and to characterize the symmetry of the state under particle exchange. The symmetry of a state in each coordinate sector is described by a Young tableau, within the convention that the state is symmetric under the exchange of two boxes in the same line and antisymmetric respect to the exchange of two boxes in the same column. The total number of boxes of the tableau is equal to the number of particles. The symmetry of the wavefunction is evaluated by computing the expectation value of the S_N class-sum operator $\Gamma_2 \doteq \sum_{a < b} P_{ab}$ on the state itself [46, 52, 53], P_{ab} being the permutation operator acting on the N particles. More in detail, P_{ab} is the operator which maps a spin sector into the one where the spins in the positions a and b are inverted. The knowledge of the class-sum operator allows us to determine the Young tableaux associated to the state. In particular, the eigenvalues γ_2 of the Γ_2 operator are linked to the Young tableaux encoding the possible symmetries of the state through the following relation:

$$\gamma_2 = \frac{1}{2} \sum_j n_j (n_j - 2j + 1), \quad (6)$$

where j labels the line of the corresponding Young tableau and n_j is the number of boxes in the j^{th} line. The eigenstates of Γ_2 are characterized by the symmetry represented by the corresponding eigenvalue. Therefore, in order to determine the symmetry of a state we evaluate its decomposition on the eigenstates of Γ_2 or, equivalently, the expectation value of Γ_2 on the state itself. If such expectation value coincides with an eigenvalue of Γ_2 , then the state has a well-defined symmetry characterized by the corresponding Young tableau. If this is not the case, the state has a mixed symmetry and the decomposition of the state on the eigenstates of Γ_2 provides the coefficients of the superposition.

3. Case of two particles

Before tackling the case of larger numbers of particle, it is instructive to understand the solution for $N = 2$ particles, i.e one boson for each component of the mixture. When $N = 2$ and $M = 1$ there are only two coordinate sectors, namely $\mathbb{1} : x_1 \leq x_2$ and $\tilde{Q} : x_2 \leq x_1$. Without loss of generality we assume the positions of the spin down particle in the two sectors to be $y_{\mathbb{1}} = 2$ and $y_{\tilde{Q}} = 1$. We use Eq. (5) to compute the amplitudes of the Bethe wavefunction:

$$\begin{aligned} A_{\mathbb{1}}(\lambda) &\propto \left(\frac{\lambda - i}{\lambda + i} \right)^2, \\ A_{\tilde{Q}}(\lambda) &\propto (-1) \left(\frac{\lambda - i}{\lambda + i} \right), \end{aligned} \quad (7)$$

where we used the property $|\mathbb{1}| = 0$ and $|\tilde{Q}| = 1$. The Bethe equation for the spin rapidity λ reads:

$$\arctan(\lambda) = \frac{\pi}{2} \mathcal{J}, \quad \mathcal{J} \in \mathbb{Z}. \quad (8)$$

In the ground state at zero flux we have $\mathcal{J} = 0$ and $A_{\mathbb{1}}(0) = A_{\tilde{Q}}(0) = 1$, while in the first excited state $\mathcal{J} = 1$ and consequently $A_{\mathbb{1}}(\infty) = 1, A_{\tilde{Q}}(\infty) = -1$. Next, in order to make a link with the standard solutions in the fermionized limit, we decompose the wavefunction in each coordinate sector on a basis of anti-symmetric combinations of plane waves, as opposed to Eq. (2). Consequently, we introduce the amplitudes $\mathcal{A} = (-1)^{|\mathbb{Q}|} A_Q$. Explicitly, the wavefunction in this form reads:

$$\Psi(x_1, x_2) = \mathcal{A}(x_1 - x_2) \det \left(e^{ik_j x_\ell} \right). \quad (9)$$

A simple reorganization of the terms entering in the above equation yields

$$\Psi(x_1, x_2) = \mathcal{A}(x_1 - x_2) \sin(k(x_1 - x_2)) e^{iK(x_1 + x_2)/2}, \quad (10)$$

where $K = k_1 + k_2$ is the center of mass momentum and $k = (k_1 - k_2)/2$ is the relative momentum of the two-particle system. In the homogeneous ring, there is complete factorization between the internal structure of the state, encoded in the term $\mathcal{A}(x_1 - x_2) \sin k((x_1 - x_2))$, where $\mathcal{A}(x_1 - x_2)$ controls the overall symmetry under exchange of particles, and the center-of-mass part $\exp(iK(x_1 + x_2)/2)$. The latter is the one which couples to the artificial gauge flux [39, 54]. The corresponding value of the energy is $E = \sum_{j=1,2} (\hbar^2/2m)[k_j - (2\pi/L)\tilde{\Phi}]^2$. The values of the wave-vectors k_1, k_2 are obtained by imposing the periodic boundary conditions $\Psi(x_1 + L, x_2) = \Psi(x_1, x_2) = \Psi(x_1, x_2 + L)$. The function $\mathcal{A}(x_1 - x_2)$ for the ground state depends on the value of the artificial gauge field.

For $-0.25 < \tilde{\Phi} < 0.25$ the ground state of distinguishable bosons coincides with the one of identical TG bosons i.e. $\mathcal{A}(x_1 - x_2) = \text{sign}(x_1 - x_2)$. In this case the periodic boundary conditions imposed on Eq.(9) yield $k_1 + k_2 = (2\pi/L)2p$ and $k_1 - k_2 = (2\pi/L)q$ with p, q integers. The solution for the ground state gives $k_1 = -\pi/L$ and $k_2 = \pi/L$.

Notice that thanks to the analogy of the Hamiltonian with the one of particles in a crystal with quasi-momentum $\tilde{\Phi}$, the same choice for $\mathcal{A}(x_1 - x_2)$ holds for all intervals of flux obtained by a translations of the interval $-0.25 < \tilde{\Phi} < 0.25$ by integer numbers, i.e shifting Φ by integer multiples of Φ_0 .

For $0.25 < \tilde{\Phi} < 0.75$ the ground state is instead obtained by choosing $\mathcal{A}(x_1 - x_2) = 1$, as for spinless fermions. This corresponds to the Bethe Ansatz solution for the wavefunction of the first excited state at zero flux. In this case, the periodic boundary conditions yield $k_1 = 0$ and $k_2 = 2\pi/L$. As above, the same choice for $\mathcal{A}(x_1, x_2)$ holds for all intervals of flux values obtained by translations of the considered interval by integer numbers.

By collecting all the above considerations, we obtain the ground-state energy as a function of flux (see Figure 1): it consists of piece-wise parabolas, with half periodicity with respect of the flux quantum Φ_0 . We notice that each parabola is associated to a different value of the total momentum $P = \hbar(k_1 + k_2)$, and hence of the total angular momentum L_z along the direction perpendicular to the ring plane, labelled by $\ell = \langle L_z \rangle / \hbar$, as also indicated on the figure, where $\langle L_z \rangle = PR$. We notice that the halved periodicity implies *fractional angular momentum per particle* as already reported for the case of attracting bosons [39], paired fermions [41, 42, 55], and SU(N) fermionic mixtures [43].

Our explicit solution allows also to readily obtain the symmetry of the ground state. For the parabola centered at zero flux (and all its translations by Φ_0), the wave-function is fully symmetric, while for the one centered at $\Phi_0/2$ (and all its translations by Φ_0) the wave-function is fully anti-symmetric. The corresponding Young Tableaux are also depicted in Figure 1.

Let us summarize the four main aspects emerging from the analysis of the two-particle case: (i) the ground state of the mixture on a ring is not degenerate, at difference from the case

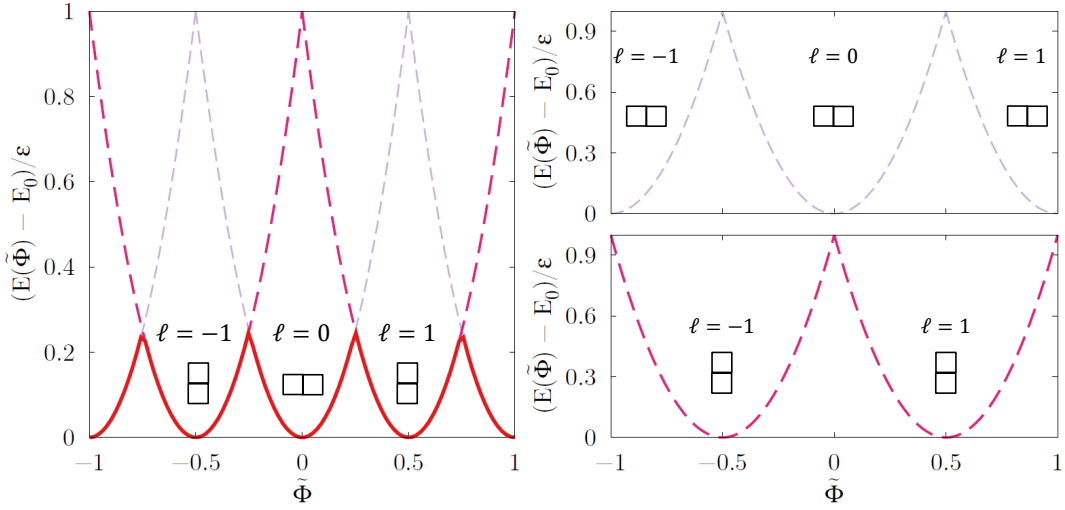


Figure 1. On the left, ground state energy (relative to the energy E_0 at zero flux, in units of ϵ) as a function of the reduced flux (dimensionless) for the case $N = 2$, $M = 1$ (red solid line). The violet and magenta dashed lines correspond to the energy landscape for $N = 2$ single-component Tonks–Girardeau bosons and spin-polarized fermions respectively. The total angular momentum quantum number and the Young tableau indicating the symmetry of the ground state under particle exchange are also indicated on each ground-state branch. On the right, we show the ground state energy as a function of the dimensionless flux for a single-component TG gas (top) and spin-polarized Fermi gas (bottom). We also report the value of the angular momentum and the Young tableau of the corresponding state.

of a mixture under harmonic confinement [18], (ii) the ground-state energy as a function of the flux is given by piece-wise parabolas, each of them characterized by a given value of total angular momentum specified by ℓ , (iii) each parabola has a well-defined symmetry (either fully symmetric or fully anti-symmetric), and (iv) the case of a two-component mixture displays a halving of the periodicity with respect to the case of a spin-polarized Fermi gas (parabolas centered at semi-integer values of Φ_0) as well as the one of a single-component TG gas (parabolas centered at integer multiples of Φ_0).

In the following, we will treat the more challenging case of a 2+2 spin mixture.

4. Results for $N = 4$, $M = 2$

In this section, we provide the results for a balanced multicomponent Bose gas of $N = 4$ particles and $M = 2$ spins down. The quantum numbers \mathcal{I}_j and \mathcal{I}_m are both semi-integers [44]. We can write Eq. (5) as follows:

$$A_Q(\lambda_1, \lambda_2) \propto (-1)^{|Q|} \left(\frac{\lambda_1 - \lambda_2 - 2i}{\lambda_1 - \lambda_2} \left(\frac{\lambda_1 - i}{\lambda_1 + i} \right)^{y_{Q(1)}} \left(\frac{\lambda_2 - i}{\lambda_2 + i} \right)^{y_{Q(2)}} + \frac{\lambda_2 - \lambda_1 - 2i}{\lambda_2 - \lambda_1} \left(\frac{\lambda_2 - i}{\lambda_2 + i} \right)^{y_{Q(1)}} \left(\frac{\lambda_1 - i}{\lambda_1 + i} \right)^{y_{Q(2)}} \right). \quad (11)$$

The set of Bethe equations is:

$$\begin{cases} Lk_j = 2\pi\mathcal{I}_j - \frac{2\pi}{4}(\mathcal{I}_1 + \mathcal{I}_2) \\ 8\arctan(\lambda_1) = 2\pi\mathcal{I}_1 - \arctan\frac{\lambda_2 - \lambda_1}{2} \\ 8\arctan(\lambda_2) = 2\pi\mathcal{I}_2 + \arctan\frac{\lambda_2 - \lambda_1}{2}, \end{cases} \quad (12)$$

Table 1. Solutions of the Bethe equations for a strongly repulsive Bose–Bose mixture of $N = 4$ particles and $M = 2$ spin-down particles. We consider various values of total angular momentum P and quantum numbers configuration $\mathcal{J}_1, \mathcal{J}_2$. Such solutions are the ground-state and the first excited states for zero reduced flux $\tilde{\Phi}$ (see column $E(0)/\epsilon$), but become the ground state in a given interval of flux as indicated in the last column of the table.

P	$\mathcal{J}_1 + \mathcal{J}_2$	$\tilde{\lambda}_1$	$\tilde{\lambda}_2$	$E(0)/\epsilon$	Reduced flux interval
0	0	$1/\sqrt{3}$	$-1/\sqrt{3}$	10	$-1/8 \leq \tilde{\Phi} \leq 1/8$
0	0	$i\infty$	$-i\infty$	10	$-1/8 \leq \tilde{\Phi} \leq 1/8$
$2\pi/L$	1	-1	∞	$21/2$	$1/8 \leq \tilde{\Phi} \leq 3/8$
$4\pi/L$	2	0	∞	12	$3/8 \leq \tilde{\Phi} \leq 5/8$
$4\pi/L$	2	i	$-i$	12	$3/8 \leq \tilde{\Phi} \leq 5/8$
$6\pi/L$	3	1	∞	$29/2$	$5/8 \leq \tilde{\Phi} \leq 7/8$

which can be simplified using the trigonometric relation $\arctan(a) + \arctan(b) = \arctan(\frac{a+b}{1-ab})$

$$\begin{cases} Lk_j = 2\pi\mathcal{J}_j - \frac{2\pi}{4}(\mathcal{J}_1 + \mathcal{J}_2) \\ \frac{\lambda_1 + \lambda_2}{1 - \lambda_1\lambda_2} = \tan\left(\frac{\pi}{4}(\mathcal{J}_1 + \mathcal{J}_2)\right) \\ 8\arctan(\lambda_2) = 2\pi\mathcal{J}_2 + \arctan\frac{\lambda_2 - \lambda_1}{2}. \end{cases} \quad (13)$$

In order to minimize the energy associated to the charge sector we have to minimize $\sum_j \mathcal{J}_j$. As a consequence, the set of quantum numbers \mathcal{J}_j for the ground state of the charge sector is $\mathcal{J}_j = \{-\frac{3}{2}, -\frac{1}{2}, \frac{1}{2}, \frac{3}{2}\}$. Moreover, due to the periodicity of the tangent function, the second equation only gives independent solutions for $(\mathcal{J}_1 + \mathcal{J}_2) \pmod{4}$. Therefore, we can focus on the four cases $\mathcal{J}_1 + \mathcal{J}_2 = 0, 1, 2, 3$, which, for each value of $\tilde{\Phi}$, correspond to respectively the ground state and the first three excited states. Explicitly, these configurations yield the following values for the total momentum $P = 0, \frac{2\pi}{L}, \frac{4\pi}{L}, \frac{6\pi}{L}$. The solutions of Eq. (13) are listed in Table 1. Remarkably, if we allow for complex λ_n , multiple solutions can be associated to the same value of the momentum. We define $a_Q^{\ell,i} = A_Q(\tilde{\lambda}_1^i(P), \tilde{\lambda}_2^i(P))$ as the amplitudes of the Bethe wavefunction for each configuration of quantum numbers and where $\tilde{\lambda}_{1,2}^i(P)$ are the i^{th} solutions of the last two Bethe equations (13) for a fixed value of the total momentum P , labelled by the quantum number ℓ . In particular, for $P = 0$ and $P = 4\pi/L$ we get two solutions, while for $P = 2\pi/L$ and $P = 6\pi/L$ the solution is unique. We also stress that in order to get all the possible low-energy excitations, we had to include singular solutions of the Bethe equations [56, 57].

Table 2. Amplitudes $a_Q^{\ell,i}$ corresponding to the different spin sectors for $N = 4$ and $M = 2$.

Sector	$a_Q^{(0,1)}$	$a_Q^{(0,2)}$	$a_Q^{(1,1)}$	$a_Q^{(2,1)}$	$a_Q^{(2,2)}$	$a_Q^{(3,1)}$
$ \uparrow\uparrow\downarrow\downarrow\rangle$	2	2	$1 - i$	0	2	$1 + i$
$ \uparrow\downarrow\uparrow\downarrow\rangle$	-4	2	0	2	0	0
$ \downarrow\uparrow\uparrow\downarrow\rangle$	2	2	$1 + i$	0	-2	$1 - i$
$ \uparrow\downarrow\downarrow\uparrow\rangle$	2	2	$-1 - i$	0	-2	$-1 + i$
$ \downarrow\uparrow\downarrow\uparrow\rangle$	-4	2	0	-2	0	0
$ \downarrow\downarrow\uparrow\uparrow\rangle$	2	2	$-1 + i$	0	2	$-1 - i$

In Table 2 we show all the possible $a_Q^{\ell,i}$ for this case in the different coordinate sectors, defined by the possible spin orderings. We get six possible solutions, which correspond to six different

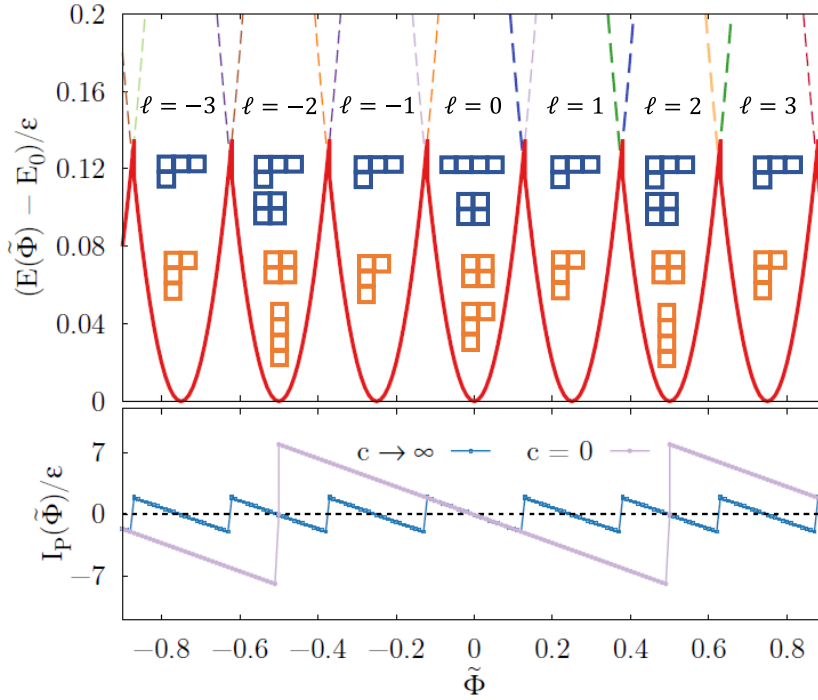


Figure 2. Top panel: energy levels (relative to the energy E_0 at zero flux, in units of ϵ) as a function of the reduced flux (dimensionless) for both a bosonic and a fermionic mixture with $N = 4$ and $M = 2$. The red continuous line highlights the ground state of the system. For each value of the flux, we indicate the angular-momentum quantum number of the ground state. The two upper lines of Young tableaux (blue diagrams) indicate the symmetry of the bosonic ground state as function of the flux. The two bottom lines (orange diagrams) the ones of the fermionic ground state. Bottom panel: corresponding persistent current, displaying the $1/N$ -periodicity emerging at strong interactions.

states. This value coincides with the possible and distinguishable spin configurations allowed in this case, given in general by $\frac{N!}{M!(N-M)!}$.

In the top panel of Figure 2 we show the energy $E(\tilde{\Phi})$ as a function of the flux. The continuous red line highlights the ground state energy, which is a periodic function of the gauge flux. Remarkably, the period is reduced by a factor of $N = 4$ if compared to the one of the non-interacting case. This effect is also reflected in the persistent current $I_P(\tilde{\Phi}) = -\frac{\partial E}{\partial \tilde{\Phi}}(\tilde{\Phi})$ evaluated in the ground state, which is shown in the bottom panel of Figure 2. We compare the persistent current for $c = 0$ and $c \rightarrow \infty$. We see the emergence of the $1/N$ -reduction of the periodicity. This effect was also reported in strongly interacting Fermi mixtures for repulsive interactions [42, 43].

Looking at Figure 2, we see that each time the flux increases by $\tilde{\Phi}/N$, the ground state carries a different value of total momentum P .

We evaluated the symmetry of the states listed in Table 2 by computing the expectation value $\langle a^{\ell,i} | \Gamma_2 | a^{\ell,i} \rangle$, $|a^{\ell,i}\rangle$ being the vector collecting the coefficients $a_Q^{\ell,i}$ in the different coordinate sectors for the i^{th} state of total momentum P (i.e the columns of Table 2), suitably normalized. For each of the above states, this expectation value coincides with an eigenvalue of the class-sum operator Γ_2 , i.e each state has well-defined symmetry. This allows us to link them to a Young tableau and therefore, for any value of the reduced flux, to determine the symmetry of the ground

state. In the top panel of Figure 2 the upper line (blue) of tableaux provides the symmetry of the ground state for each branch of the ground-state energy as a function of the flux.

It is instructive to compare our results for the Bose–Bose mixture with the ones for a Fermi–Fermi mixture with repulsive contact inter-component interactions. In this case, the wavefunction has still the form Eq. (2). However, the Bethe equations are different since there is no contact interactions among fermions belonging to the same component, and also the symmetry under exchange of particles belonging to the same component is different. At strong repulsive interactions the first of Bethe equations (4) reads $Lk_j = 2\pi(\mathcal{I}_j + \frac{1}{N}\sum_{m=1}^M \mathcal{I}_m)$ while the equation for the spin rapidities coincide to the one for the bosonic case [42, 43]. The results for the solutions of the Bethe equations for the fermionic case are summarized in Table 3. In this case the quantum numbers \mathcal{I}_j for $N = 4$ and $M = 2$ are integers [16]. In the ground state, we have $\mathcal{I}_j = \{-2, -1, 0, 1\}$ which implies $\sum_j \mathcal{I}_j = -2$. The total momentum is $P_F = \frac{2\pi\hbar}{L}(\sum_j \mathcal{I}_j + \sum_a \mathcal{I}_a) \doteq \frac{\hbar}{R} \ell_F$ [43, 47, 48]. The energy levels as a function of the flux are the same as for the Bose–Bose mixture. Similarly, for a given value of $\tilde{\Phi}$, the angular momentum of the ground state is the same for bosons and fermions.

On the other hand, the symmetry of the ground state is markedly different in the two cases. We evaluate the symmetry of the fermionic ground-state wavefunction by following the same procedure used for the bosonic system. Since the Bethe equation for the spin rapidities is the same as in the bosonic case, the fermionic amplitudes satisfy $a_Q^{\ell_F, j} = a_Q^{(\ell-2)(\text{mod } 4), j}$, where ℓ_F labels fermionic states with different angular momentum. As a consequence, the same value of the total momentum P_F is associated to different spin rapidities in the two cases and therefore to different amplitudes A_Q . As the amplitudes affect the symmetry of the wave-function, the corresponding Young tableaux are different in the fermionic and in the bosonic case. The Young tableaux indicating the symmetries of the fermionic ground state as a function of the flux are displayed in orange in the top panel of Figure 2.

We also remark that – both in the case of bosonic and fermionic mixtures – different parabolas display different symmetries, reflecting the fact that they correspond to different excited states at zero flux.

Let us insist that these features are due to the fact that we are considering a two-component system, where different symmetries are possible. We remind that for the case of a single-component gas, also for the case of $N = 4$ particles, the energy landscapes are those shown in the right panels of Figure 1 (top panel for the TG gas and bottom panel for spinless fermions).

Table 3. Solutions of the Bethe equations for a strongly repulsive Fermi–Fermi mixture for $N = 4$, $M = 2$ and for various values of total momentum P_F . We also provide the energy associated to each state at zero flux and the reduced flux interval where each state becomes the ground state.

P_F	$\mathcal{I}_1 + \mathcal{I}_2$	$\tilde{\lambda}_1$	$\tilde{\lambda}_2$	$E(0)/\epsilon$	Reduced flux interval
0	2	0	∞	10	$-1/8 \leq \tilde{\Phi} \leq 1/8$
0	2	i	$-i$	10	$-1/8 \leq \tilde{\Phi} \leq 1/8$
$2\pi/L$	3	1	∞	$21/2$	$1/8 \leq \tilde{\Phi} \leq 3/8$
$4\pi/L$	4	$\frac{1}{\sqrt{3}}$	$-\frac{1}{\sqrt{3}}$	12	$3/8 \leq \tilde{\Phi} \leq 5/8$
$4\pi/L$	4	∞	∞	12	$3/8 \leq \tilde{\Phi} \leq 5/8$
$6\pi/L$	5	-1	∞	$29/2$	$5/8 \leq \tilde{\Phi} \leq 7/8$

5. Summary and conclusions

We have studied the ground-state properties of a strongly interacting Bose–Bose mixture subjected to an artificial gauge field on a ring. We have found that the ground-state energy is a periodic function of the flux, made by piece-wise parabolas. As compared to the case of non interacting particles, the period of the ground-state energy, as well as the one of the persistent current, is reduced by a factor N , with N the total number of particles in the mixture. We understand the reduction of periodicity as being due to spin excitations, according to the following mechanism: in the absence of artificial gauge field, the spin excitations lie above the ground state. However, the application of a gauge field decreases the values of the energy of such spin-excited states, making them become the ground state in some intervals of reduced flux.

Each parabola of the ground-state energy landscape is associated to a value of the total angular momentum which increases by one quantum by moving from one parabola to the next. Hence, the emergence of such new branches corresponds to states with fractional angular momentum per particle. This phenomenon was previously reported for the case of Fermi mixtures with strong repulsive interactions - our analysis proposes yet another system where this same effect occurs.

Furthermore, we have characterized the symmetry under exchange of particles of such ground-state branches as a function of the flux, and shown that a single Young tableau can be associated to each branch when it is non-degenerate, while more than one tableau is found when the ground state is degenerate. This analysis confirms the role of spin excitations as being responsible of the reduction of periodicity and the emergence of the new parabolic branches which are absent in the non-interacting regime.

The $1/N$ - angular-momentum fractionalization was also found for multicomponent Fermi gases at large but finite repulsive interactions [42, 43]. Such regime could be accessed by performing a perturbative expansion of the Bethe Ansatz solution to first order in $1/c$.

Our study contributes to the deep understanding of the spectrum structure and opens the possibility of designing experiments in which particular symmetries, i.e particular spin states, can be selected. This could be done by applying an artificial gauge flux whose value is within the interval where the ground state is associated to the designated symmetry or superposition of different symmetries. An experimental way to access to the symmetries would be to measure the Tan's contact of the mixture [58].

Conflicts of interest

The authors have no conflict of interest to declare.

Acknowledgements

A.M. and G.P. acknowledge fruitful discussions with L. Amico.

References

- [1] I. Bloch, J. Dalibard, W. Zwerger, “Many-body physics with ultracold gases”, *Rev. Mod. Phys.* **80** (2008), no. 3, p. 885-964.
- [2] C. Gross, I. Bloch, “Quantum simulations with ultracold atoms in optical lattices”, *Science* **357** (2017), no. 6355, p. 995-1001.
- [3] M. Lewenstein, A. Sanpera, V. Ahufinger, *Ultracold Atoms in Optical Lattices: Simulating quantum many-body systems*, OUP Oxford, 2012.
- [4] C. Chin, R. Grimm, P. Julienne, E. Tiesinga, “Feshbach resonances in ultracold gases”, *Rev. Mod. Phys.* **82** (2010), no. 2, p. 1225-1286.

- [5] F. Serwane, G. Zürn, T. Lompe, T. B. Ottenstein, A. N. Wenz, S. Jochim, “Deterministic Preparation of a Tunable Few-Fermion System”, *Science* **332** (2011), no. 6027, p. 336-338.
- [6] B. Paredes, A. Widera, V. Murg, O. Mandel, S. Fölling, I. Cirac, G. V. Shlyapnikov, T. W. Hänsch, I. Bloch, “Tonks–Girardeau gas of ultracold atoms in an optical lattice”, *Nature* **429** (2004), no. 6989, p. 277-281.
- [7] T. Kinoshita, T. Wenger, D. S. Weiss, “Observation of a One-Dimensional Tonks-Girardeau Gas”, *Science* **305** (2004), no. 5687, p. 1125-1128.
- [8] T. Kinoshita, T. Wenger, D. S. Weiss, “A quantum Newton’s cradle”, *Nature* **440** (2006), no. 7086, p. 900-903.
- [9] S. I. Mistakidis, A. G. Volosniev, R. E. Barfknecht, T. Fogarty, T. Busch, A. Foerster, P. Schmelcher, N. T. Zinner, “Cold atoms in low dimensions – a laboratory for quantum dynamics”, *preprint*, arXiv:2202.11071, 2022.
- [10] E. H. Lieb, W. Liniger, “Exact Analysis of an Interacting Bose Gas. I. The General Solution and the Ground State”, *Phys. Rev.* **130** (1963), no. 4, p. 1605-1616.
- [11] C. N. Yang, “Some Exact Results for the Many-Body Problem in one Dimension with Repulsive Delta-Function Interaction”, *Phys. Rev. Lett.* **19** (1967), no. 23, p. 1312-1315.
- [12] M. Gaudin, *The Bethe Wavefunction*, Cambridge University Press, 2014.
- [13] B. Sutherland, “Further Results for the Many-Body Problem in One Dimension”, *Phys. Rev. Lett.* **20** (1968), no. 3, p. 98-100.
- [14] B. Sutherland, “Model for a multicomponent quantum system”, *Phys. Rev. B* **12** (1975), no. 9, p. 3795-3805.
- [15] B. Sutherland, *Beautiful models: 70 years of exactly solved quantum many-body problems*, World Scientific, 2004.
- [16] N. Oelkers, M. T. Batchelor, M. Bortz, X.-W. Guan, “Bethe ansatz study of one-dimensional Bose and Fermi gases with periodic and hard wall boundary conditions”, *J. Phys. A, Math. Gen.* **39** (2006), no. 5, p. 1073-1098.
- [17] A. Minguzzi, P. Vignolo, “Strongly interacting trapped one-dimensional quantum gases: Exact solution”, *AVS Quantum Sci.* **4** (2022), no. 2, article no. 027102.
- [18] A. G. Volosniev, D. V. Fedorov, A. S. Jensen, M. Valiente, N. T. Zinner, “Strongly interacting confined quantum systems in one dimension”, *Nat. Commun.* **5** (2014), no. 1, article no. 5300.
- [19] F. Deuretzbacher, D. Becker, J. Bjerlin, S. M. Reimann, L. Santos, “Quantum magnetism without lattices in strongly interacting one-dimensional spinor gases”, *Phys. Rev. A* **90** (2014), no. 1, article no. 013611.
- [20] L. Amico, M. Boshier, G. Birkl, A. Minguzzi, C. Miniatura, L.-C. Kwek, D. Aghamalyan, V. Ahufinger, D. Anderson, N. Andrei *et al.*, “Roadmap on Atomtronics: State of the art and perspective”, *AVS Quantum Sci.* **3** (2021), no. 3, article no. 039201.
- [21] J. Dalibard, “Introduction to the physics of artificial gauge fields”, in *Lecture notes of the International School of Physics “Enrico Fermi” on Quantum Matter at Ultralow Temperatures (Varenna 7 - 15 July 2014)* (M. Inguscio, W. Ketterle, S. Stringari *et al.*, eds.), IOS Press, 2016, p. 1-61.
- [22] J. Dalibard, F. Gerbier, G. Juzelinis, P. Öhberg, “Colloquium: Artificial gauge potentials for neutral atoms”, *Rev. Mod. Phys.* **83** (2011), no. 4, p. 1523-1543.
- [23] N. Goldman, G. Juzeliūnas, P. Öhberg, I. B. Spielman, “Light-induced gauge fields for ultracold atoms”, *Rep. Prog. Phys.* **77** (2014), no. 12, article no. 126401.
- [24] K. C. Wright, R. B. Blakestad, C. J. Lobb, W. D. Phillips, G. K. Campbell, “Driving Phase Slips in a Superfluid Atom Circuit with a Rotating Weak Link”, *Phys. Rev. Lett.* **110** (2013), no. 2, article no. 025302.
- [25] A. Kumar, R. Dubessy, T. Badr, C. De Rossi, M. de Goër de Herve, L. Longchambon, H. Perrin, “Producing superfluid circulation states using phase imprinting”, *Phys. Rev. A* **97** (2018), no. 4, article no. 043615.
- [26] A. A. Zvyagin, I. V. Krive, “Persistent currents in one-dimensional systems of strongly correlated electrons”, *Low Temperature Physics* **21** (1995), p. 533-555.
- [27] S. Viefers, P. Koskinen, P. Singha Deo, M. Manninen, “Quantum rings for beginners: energy spectra and persistent currents”, *Physica E Low Dimens. Syst. Nanostruct.* **21** (2004), no. 1, p. 1-35.
- [28] L. Amico, D. Anderson, M. Boshier, J.-P. Brantut, L.-C. Kwek, A. Minguzzi, W. von Klitzing, “Colloquium: Atomtronic circuits: from many-body physics to quantum technologies”, *Rev. Mod. Phys.* **94** (2022), article no. 041001.
- [29] L. Amico, A. Osterloh, F. Cataliotti, “Quantum Many Particle Systems in Ring-Shaped Optical Lattices”, *Phys. Rev. Lett.* **95** (2005), no. 6, article no. 063201.
- [30] A. Richaud, M. Ferraretto, M. Capone, “Interaction-resistant metals in multicomponent Fermi systems”, *Phys. Rev. B* **103** (2021), no. 20, article no. 205132.
- [31] S. Eckel, F. Jendrzejewski, A. Kumar, C. J. Lobb, G. K. Campbell, “Interferometric Measurement of the Current-Phase Relationship of a Superfluid Weak Link”, *Phys. Rev. X* **4** (2014), no. 3, article no. 031052.
- [32] L. Corman, L. Chomaz, T. Bienaimé, R. Desbuquois, C. Weitenberg, S. Nascimbène, J. Dalibard, J. Beugnon, “Quench-Induced Supercurrents in an Annular Bose Gas”, *Phys. Rev. Lett.* **113** (2014), no. 13, article no. 135302.
- [33] R. Mathew, A. Kumar, S. Eckel, F. Jendrzejewski, G. K. Campbell, M. Edwards, E. Tiesinga, “Self-heterodyne detection of the in situ phase of an atomic superconducting quantum interference device”, *Phys. Rev. A* **92** (2015), no. 3, article no. 033602.
- [34] Y. Cai, D. G. Allman, P. Sabharwal, K. C. Wright, “Persistent Currents in Rings of Ultracold Fermionic Atoms”, *Phys. Rev. Lett.* **128** (2022), no. 15, article no. 150401.

- [35] G. Del Pace, K. Khani, A. M. Falconi, M. Fedrizzi, N. Grani, D. H. Rajkov, M. Inguscio, F. Scazza, W. J. Kwon, G. Roati, “Imprinting persistent currents in tunable fermionic rings”, *Phys. Rev. X* **12** (2022), no. 4, article no. 041037.
- [36] W. J. Chetcuti, A. Osterloh, L. Amico, J. Polo, “Interference dynamics of matter-waves of $SU(N)$ fermions”, *preprint*, arXiv:2206.02807, 2022.
- [37] N. Byers, C. N. Yang, “Theoretical Considerations Concerning Quantized Magnetic Flux in Superconducting Cylinders”, *Phys. Rev. Lett.* **7** (1961), no. 2, p. 46-49.
- [38] A. J. Leggett, “Some Considerations Related to the Quantization of Charge in Mesoscopic Systems”, in *Granular Nanoelectronics* (C. W. J. Beenakker *et al.*, eds.), NATO Science Series B: Physics, vol. 251, Plenum Press, New York, 1991, p. 343-358.
- [39] P. Naldesi, J. Polo, V. Dunjko, H. Perrin, M. Olshanii, L. Amico, A. Minguzzi, “Enhancing sensitivity to rotations with quantum solitonic currents”, *SciPost Phys.* **12** (2022), article no. 138.
- [40] X. Waintal, G. Fleury, K. Kazymyrenko, M. Houzet, P. Schmitteckert, D. Weinmann, “Persistent Currents in One Dimension: The Counterpart of Leggett’s Theorem”, *Phys. Rev. Lett.* **101** (2008), no. 10, article no. 106804.
- [41] G. Pecci, P. Naldesi, L. Amico, A. Minguzzi, “Probing the BCS-BEC crossover with persistent currents”, *Phys. Rev. Res.* **3** (2021), no. 3, article no. L032064.
- [42] N. Yu, M. Fowler, “Persistent current of a Hubbard ring threaded with a magnetic flux”, *Phys. Rev. B* **45** (1992), no. 20, p. 11795-11804.
- [43] W. J. Chetcuti, T. Haug, L.-C. Kwek, L. Amico, “Persistent current of $SU(N)$ fermions”, *SciPost Phys.* **12** (2022), article no. 033.
- [44] Y.-Q. Li, S.-J. Gu, Z.-J. Ying, U. Eckern, “Exact results of the ground state and excitation properties of a two-component interacting Bose system”, *Eur. Phys. Lett.* **61** (2003), no. 3, p. 368-374.
- [45] A. Imambekov, E. Demler, “Exactly solvable case of a one-dimensional Bose–Fermi mixture”, *Phys. Rev. A* **73** (2006), no. 2, article no. 021602.
- [46] A. Imambekov, E. Demler, “Applications of exact solution for strongly interacting one-dimensional Bose–Fermi mixture: Low-temperature correlation functions, density profiles, and collective modes”, *Ann. Phys.* **321** (2006), no. 10, p. 2390-2437.
- [47] F. H. L. Essler, H. Frahm, F. Göhmann, A. Klümper, V. E. Korepin, *The One-Dimensional Hubbard Model*, Cambridge University Press, 2005.
- [48] M. Ogata, H. Shiba, “Bethe-ansatz wave function, momentum distribution, and spin correlation in the one-dimensional strongly correlated Hubbard model”, *Phys. Rev. B* **41** (1990), no. 4, p. 2326-2338.
- [49] H. Bethe, “Zur theorie der metalle. I. Eigenwerte und Eigenfunktionen der linearen Atomkette”, *Z. Phys.* **71** (1931), no. 3, p. 205-226.
- [50] F. Franchini *et al.*, *An introduction to integrable techniques for one-dimensional quantum systems*, Springer, 2017.
- [51] M. Girardeau, “Relationship between Systems of Impenetrable Bosons and Fermions in One Dimension”, *J. Math. Phys.* **1** (1960), no. 6, p. 516-523.
- [52] J. Decamp, P. Armagnat, B. Fang, M. Albert, A. Minguzzi, P. Vignolo, “Exact density profiles and symmetry classification for strongly interacting multi-component Fermi gases in tight waveguides”, *New J. Phys.* **18** (2016), no. 5, article no. 055011.
- [53] N. Andrei, K. Furuya, J. H. Lowenstein, “Solution of the Kondo problem”, *Rev. Mod. Phys.* **55** (1983), no. 2, p. 331-402.
- [54] M. Manninen, S. Viefers, S. M. Reimann, “Quantum rings for beginners II: Bosons versus fermions”, *Physica E Low Dimens. Syst. Nanostruct.* **46** (2012), p. 119-132.
- [55] F. Bloch, “Superfluidity in a Ring”, *Phys. Rev. A* **7** (1973), no. 6, p. 2187-2191.
- [56] R. I. Nepomechie, C. Wang, “Algebraic Bethe ansatz for singular solutions”, *J. Phys. A, Math. Theor.* **46** (2013), no. 32, article no. 325002.
- [57] A. N. Kirillov, R. Sakamoto, “Singular solutions to the Bethe ansatz equations and rigged configurations”, *J. Phys. A, Math. Theor.* **47** (2014), no. 20, article no. 205207.
- [58] J. Decamp, J. Jünemann, M. Albert, M. Rizzi, A. Minguzzi, P. Vignolo, “High-momentum tails as magnetic-structure probes for strongly correlated $SU(\kappa)$ fermionic mixtures in one-dimensional traps”, *Phys. Rev. A* **94** (2016), no. 5, article no. 053614.